Journal of Structural Biology 197 (2017) 220–226

Contents lists available at ScienceDirect

Journal of Structural Biology

journal homepage: www.elsevier.com/locate/yjsbi

Blotting-free and lossless cryo-electron microscopy grid preparation from nanoliter-sized protein samples and single-cell extracts

Stefan A. Arnold [a,b], Stefan Albiez [a], Andrej Bieri [a], Anastasia Syntychaki [a], Ricardo Adaixo [a], Robert A. McLeod [a], Kenneth N. Goldie [a], Henning Stahlberg [a], Thomas Braun [a,*]

[a] Center for Cellular Imaging and NanoAnalytics (C-CINA), Biozentrum, University of Basel, Switzerland
[b] Swiss Nanoscience Institute, University of Basel, Switzerland

ARTICLE INFO

Article history:
Received 17 August 2016
Received in revised form 24 October 2016
Accepted 14 November 2016
Available online 15 November 2016

Keywords:
Cryo electron microscopy
Sample preparation
Microfluidics

ABSTRACT

We present a sample preparation method for cryo-electron microscopy (cryo-EM) that requires only 3–20 nL of sample to prepare a cryo-EM grid, depending on the protocol used. The sample is applied and spread on the grid by a microcapillary. The procedure does not involve any blotting steps, and real-time monitoring allows the water film thickness to be assessed and decreased to an optimum value prior to vitrification. We demonstrate that the method is suitable for high-resolution cryo-EM and will enable alternative electron microscopy approaches, such as single-cell visual proteomics.

1. Introduction

In recent years, transmission electron microscopy (TEM) of vitrified specimens (cryo-EM; Dubochet et al., 1988) has become a powerful technique for the high-resolution structural analysis of biological matter (Liao et al., 2013), and is now increasingly recognized as a mainstream tool in biology (Callaway, 2015; Kuhlbrandt, 2014; Nogales, 2015). Several technical achievements have made this development possible, the most prominent being the recent introduction of direct electron detection (DED) cameras (Milazzo et al., 2011; Ruskin et al., 2013; Veesler et al., 2013), and the availability of improved data processing algorithms (Grigorieff, 2007; Lyumkis et al., 2013; Scheres, 2012).

Cryogenic sample-grid (cryo-EM grid) preparation and imaging methods ensure that biological specimens withstand the ultra-high vacuum inside electron microscopes, allow their investigation while trapped at physiological conditions that conserve the structural arrangement of the biomolecules and reduce the effect of radiation damage (Baker and Rubinstein, 2010; Dubochet et al., 1988; Lepault et al., 1983). However, these preparation methods have not improved significantly over the last 20 years and have some major drawbacks: a 2–4 μL sample volume is required, and 99.9% of the sample volume is lost during grid preparation, due to an extensive blotting step made with filter paper (Kemmerling et al., 2012). Furthermore, blotting with filter paper can lead to protein aggregation or denaturation. The current state of the art sample preparation methods are recognized as one of the most significant limitations in cryo-EM (Glaeser, 2016).

Improved cryo-EM grid preparation strategies that reduce sample consumption are now an essential requirement. A device that combines ink-jet picoliter dispensing with a plunge-freezing apparatus was presented in 2012 (Jain et al., 2012), and was recently refined by the use of self-blotting grids to allow cryo-grid preparation in combination with ink-jet spotting (Razinkov et al., 2016). Here, we present a paper blotting- and spotting-free method that requires total sample volumes of just a few nanoliters (e.g., 3–20 nL). It uses a microcapillary to directly 'write' the sample on holey carbon EM grids and subsequently vitrifies the deposited liquid, producing thin layers of vitrified specimen in the holes of the carbon film.

2. Material and methods

The instrument presented here is described in the Section 3. Additional aspects were published previously, such as the conditioning and preparation of nanoliter volumes for negative stain EM, or the single-cell lysis and aspiration device using a microcapillary electrode (Arnold et al., 2016; Kemmerling et al., 2013). Supporting Information S1 provides a detailed description of the

* Corresponding author at: C-CINA, Biozentrum, University of Basel, Mattenstrasse 26, CH-4058 Basel, Switzerland.
E-mail address: thomas.braun@unibas.ch (T. Braun).

http://dx.doi.org/10.1016/j.jsb.2016.11.002
1047-8477/

setup, including a parts lists and details of the method. Supporting Information S2 describes the control software.

2.1. Chemicals and buffers

All chemicals were ordered from Sigma-Aldrich, Switzerland if not otherwise indicated. The following buffers were used: *PBS*, Dulbecco's Phosphate Buffered Saline, 2.7 mM KCl, 1.5 mM KH_2PO_4, 136.9 mM NaCl, 8.9 mM $Na_2HPO_4{\cdot}7H_2O$, pH 7.4; *Tris-HCl buffer*, 20 mM Tris-HCl, 50 mM NaCl (pH 7.4); *HEPES buffer*, 10 mM HEPES pH 8.0, 50 mM KCl.

2.2. Test samples

The test samples were (i) tobacco mosaic virus (TMV) in PBS containing 0.1% decyl-β-D-maltopyranoside (DM, Anatrace), (ii) a mixture containing apoferritin and phages against *Escherichia coli* (vB_EcoM_CBA120) in Tris-HCl buffer, and (iii) a purified 200 kDa membrane protein (name not disclosed) reconstituted in amphipols. In this case, the bulk membrane protein sample was applied to a S200 10/300GL size exclusion chromatography column equilibrated with HEPES buffer complemented with 5 μM sodium azide. A single 300 μl fraction corresponding to the center of the major A280 peak was used to prepare cryo-EM grids (a) by using the cryoWriter and (b) by using a Vitrobot IV plunge-freezer (FEI, USA). The protein concentration of this fraction was 0.35 mg/mL as determined by absorbance measurement using an UV–vis spectrophotometer (Nanodrop 2000, Thermo Fisher Scientific Inc.) and assuming Abs (0.1%) = 1. (iv) Urease from *Yersinia enterocolitica* bacteria at a concentration of 0.35 mg/mL in PBS buffer.

2.3. EM grids

Various EM grids were used with the cryoWriter, such as 200-mesh copper grids with holey carbon film (R2/2, R2/1, and R1.2/1.3, Quantifoil, Germany), as well as holey carbon grids with an additional layer of continuous carbon, and lacey carbon grids. EM grids were glow discharged for 30 s in air plasma immediately before use. Note that the flatness of the grid is an important aspect, both for the mechanical writing step and for efficient heat-transfer when the grid is on the temperature controlled dew point stage (DP-stage) of the cryoWriter.

2.4. Cryo-grid preparation

The two deposition protocols used with the cryoWriter setup are detailed in the sections below and in Supporting Information S1.

2.5. Electron microscopy and single particle analysis

Unless otherwise specified, the EM grids with test samples were placed in a Gatan-626 cryo-holder and imaged in a Philips CM200 (FEG) TEM operated at 200 kV and equipped with a TVIPS F416 4k CMOS camera (TVIPS, Germany).

Images of urease for single particle analysis were acquired using a FEI Titan Krios, operated at 300 kV and equipped with Gatan Quantum-LS (zero-loss slit width of 20 eV) and Gatan K2 Summit DED camera. Low dose conditions were applied with a total electron dose of ~50 e^-/A^2 at a dose rate of 5–6 e^-/physical-pixel/s for a stack of 40 images obtained in movie mode. Drift- and contrast transfer function (CTF) correction was applied to the urease data with the Zorro software (McLeod et al., submitted) using CTFFIND4 (Rohou and Grigorieff, 2015). Approximately 10,000 particles were manually selected from the 51 micrographs recorded using EMAN2 (Tang et al., 2007) and subsequently processed in RELION-1.4 (Scheres, 2012). After particle alignment, around 8700 particles yielded good 2D class averages that were subsequently used for the 3D classification. The two best 3D classes were selected (containing ~7800 particles) and iteratively refined. A final sharpening of the map was then performed, yielding the final 3D reconstruction of the urease complex. The atomic model (PDB: 10.2210/pdb4z42/pdb) was fitted into the 3D map using the UCSF chimera software (Pettersen et al., 2004).

3. Results

3.1. Principles and setup

The cryoWriter setup and the principles of the method are depicted in Fig. 1; further details can be found in Supporting Information S1 and S2. The cryoWriter is integrated into a liquid handling and transfer system developed previously for nanoliter-volume sample conditioning and EM grid preparation for negative stain and trehalose embedding (Arnold et al., 2016) and is not enclosed in a humidity-controlled environment. The method uses a high-precision pipetting system to control liquid uptake and dispensing by a microcapillary, a temperature-controlled DP-stage to control the environment of the EM grid, a real-time monitoring system to control the thickness of the sample layer, and a pick-and-plunge-mechanism for sample vitrification. The entire process is controlled by an openBEB (Ramakrishnan et al., 2014) plug-in developed in LabVIEW (Elliott et al., 2007) and can be automated using macros (see Supporting Information S2).

The setup for cryo-grid preparation and the basic procedure (Fig. 1) are as follows: (i) *Grid cooling*: a glow-discharged standard holey carbon film EM grid held by tweezers is positioned on the cold DP-stage. (ii) *Sample up-take*; a microcapillary and high-precision pump system are used to aspirate a liquid plug from a sample stock or the lysate of a single cell immediately after electrolysis, as described previously (Arnold et al., 2016; Kemmerling et al., 2013). (iii) *Sample deposition* (Fig. 1a), the microcapillary tip is brought into close proximity of the grid surface. The sample is then dispensed from the microcapillary to form a small liquid droplet that spans the gap between the microcapillary tip and the hydrophilic (glow-discharged) holey-carbon surface of the EM grid. Simultaneously, the grid is moved relative to the nozzle in a sinusoidal or circular pattern; the liquid sample is spread-out over the surface filling the holes of the carbon film. (iv) *Sample stabilization and thinning* by controlled water evaporation (Fig. 1b and dedicated section below); the temperature of the DP-stage is set to keep both the EM grid and the suspended sample at a specified temperature close to the dew-point temperature of the room, throughout. Note that the grid is not immediately vitrified, but can be kept on the stage for a short time (between <1 and 10 s, depending on the chosen offset temperature), so that a certain amount of sample water can evaporate. Interference/scattering effects from interaction of the grid and applied aqueous sample with a 780 nm laser beam can be used to monitor the evaporation (Fig. 2). The controlled loss of some water is important to ensure that a thin water film spans the holes of the carbon layer. (v) *Cryo-grid pick-and-plunge freezing* (Fig. 1c); the mechanism is triggered by the monitoring system or after a pre-set time, rapidly plunging the grid (and tweezer tips) into a liquid ethane/propane (40:60) bath (Tivol et al., 2008) for vitrification (see also Supporting Information S1 and Supplementary Movie 1).

Two deposition protocols can be used with this basic procedure, depending on the experiment and sample. In Protocol 1, a relatively large volume (20 nL) is deposited on the grid, excess sample is removed and recovered by re-aspiration with the dispensing microcapillary; this protocol is ideal for the preparation of large

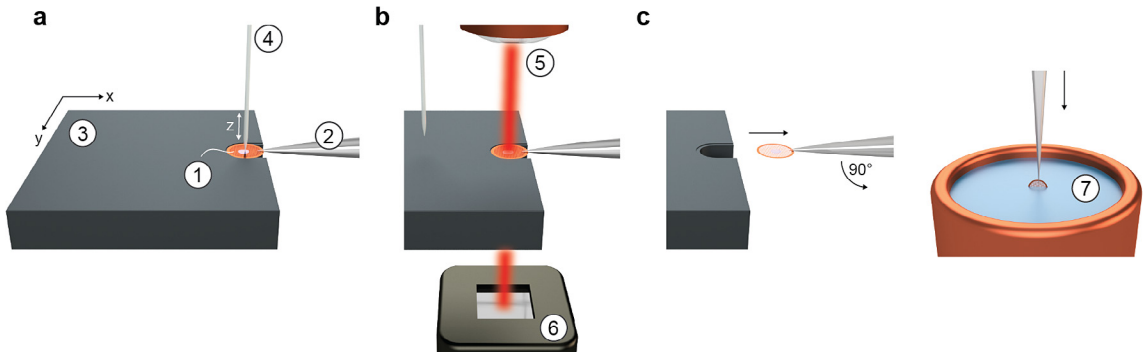

Fig. 1. Working principle of the cryoWriter device. For further details, see Supporting Information S1–S2. (a) A standard holey carbon film EM grid (1) is mounted between the tips of tweezers (2) and positioned flat (horizontal) in a slot in a temperature-controlled dew point stage (DP-stage) (3). The DP-stage temperature is set close to the dew point temperature and can be regulated using a PID Peltier controller. The EM grid is in good thermal contact with the stage. The DP-stage (3) is mounted on a motorized xy axis to move the grid relative to a microcapillary (4), which can be lowered to a few micrometers above the grid. This microcapillary deposits a few nanoliters of sample while the stage is moving in a sinuous pattern, covering an area of about 0.5 mm^2. (b) After sample deposition, the microcapillary is withdrawn and the stage (3) moves to position the grid (1) between an IR laser (λ = 780 nm; 5) and a photodiode (6). Light scattering and interference effects from the thin aqueous sample film on the grid change as water evaporates (see Fig. 2 and Supporting Information S3). (c) A trigger automatically initiates plunge-freezing when the photodiode signal reaches a defined threshold level. The tweezers and grid are rapidly withdrawn from the stage, flipped by 90 degrees into the vertical position and plunged into a cryogen (7). This whole pick-and-plunge process takes a few hundred milliseconds. See Supporting Movie 1.

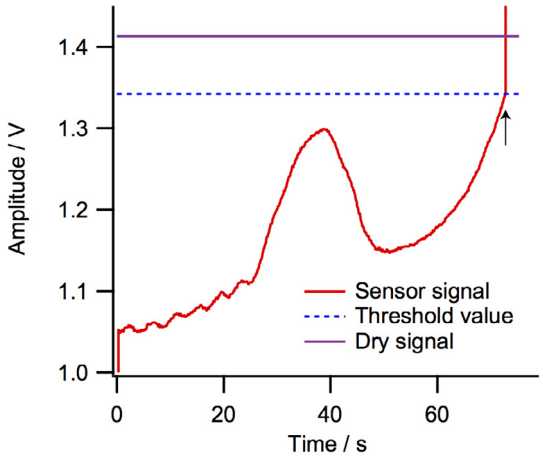

Fig. 2. Real-time monitoring of water evaporation from the sample to control the thickness of the vitreous ice layer. The transmitted light of a 780 nm laser is used to register changes in the water-layer thickness before vitrification (see Fig. 1b). The purple (static) line is the signal obtained with the dry grid (dry signal). The red line is the sensor signal recorded after sample deposition during water evaporation (stage temperature 2 °C above the dew point). Empirically, it was found that useable grids are obtained when the sensor signal is about 95% (blue line) of the dry signal. The pick-and-plunge mechanism is triggered when this threshold is reached (indicated by an arrow), leading to the rapid vitrification of the cryo-EM grid (within a few hundred milliseconds). The plot shows the characteristic evolution of the signal over time as sample water evaporates and the very steep increase that occurs as the grid is removed from the optical laser-path (arrow). This graph was chosen for clarity, as it shows a large volume (20 nL) evaporating for a long time at a small offset from the dew point (2 °C). In reality, less sample is deposited (or sample is re-aspirated beforehand), and only the last few seconds of the plot can be recorded.

EM imaging areas of purified protein complexes for single-particle analysis and high-resolution structure determination. In Protocol 2, a ~3 nL sample volume is directly deposited on the grid, avoiding the need for a re-aspiration step. This protocol is better suited for applications that are restricted to minute volumes, e.g., single-cell visual proteomics (Arnold et al., 2016; Engel, 2010; Kemmerling et al., 2012). These protocols are described in detail below.

3.1.1. Protocol 1: Deposition with recovery of excess sample

The microcapillary and the high-precision pump system are used to aspirate a few tens of nanoliters from a sample stock. The microcapillary tip is then lowered to the glow-discharged grid surface (separation ~10 µm) and a 20 nL drop of sample is dispensed from it. The drop spans the gap between the microcapillary tip and the EM grid and can be spread further to cover an area of ~0.5 mm^2 by moving the grid relative to the microcapillary (Fig. 1a). Subsequently, the microcapillary tip is lowered to touch the grid surface within this area and re-aspirate as much excess sample as possible, recovering this for future use. The temperature of the DP-stage (and the grid) is kept above the dew-point temperature of the room for all of these steps, to allow a minimal amount of water to evaporate. A temperature offset from the dew point of +8 °C, combined with immediate plunge-freezing after re-aspiration of excess sample, typically results in a good sample thickness for high-resolution structural analysis. If more precision is required, the thickness of the sample film can be optimized by controlled water evaporation using the real-time monitoring system described below. A more extensive discussion of the sample thinning process can be found in the dedicated Section 3.2.

3.1.2. Protocol 2: Direct sample deposition without re-aspiration

With this protocol, ~3 nL of sample are directly deposited onto the grid, avoiding the re-aspiration step. The grid temperature is kept at the dew point to avoid water evaporation, and the tiny sample droplet is spread by moving the EM grid underneath the microcapillary tip in a sinusoidal or circular pattern covering an area of approx. 0.5 mm^2. Subsequently, a sample-thinning step must be performed by controlled water evaporation before plunge-freezing. Evaporation is induced by increasing the DP-stage temperature to a value slightly above the dew point of the room (e.g., +2 °C). To obtain reproducible results with these small volumes, the sample thinning process must be supervised by the monitoring system (see dedicated section).

3.2. Sample stabilization and thinning by controlled water evaporation

Due to surface tension effects, even extremely small sample aliquots must be thinned for the grids to be usable for cryo-EM. Recently, an interesting method was demonstrated using "self-blotting" grids in combination with ink-jet spotting (Razinkov et al., 2016). Here, we propose a method based on the controlled evaporation of sample water to create thin sample layers. Sample film thickness can be tuned by adjusting the temperature of the DP-stage and the time span before pick-and-plunge-freezing

is initiated (see also Supporting Information S3, section I). The sample is concentrated by water evaporation. This might be desirable for the protein, but salt concentrations also increase, which can potentially harm protein complexes. Thus, thinning in this way is limited to sample films that are already thin, making the re-aspiration of samples prepared by deposition protocol 1 essential, as demonstrated by Supporting Information S4. Note that, if necessary, the liquid handling and transfer system supporting the cryoWriter would allow sample conditioning, e.g., salt exchange by a diffusion driven process (Arnold et al., 2016) before cryo-grid preparation.

The cryoWriter setup includes a laser diode (780 nm; Fig. 1b) and a photo detector to follow the evaporation of sample liquid from the grid in real-time. At 780 nm wavelength, light is not significantly absorbed by water or biological material, making the amount of heat transferred to the sample negligible (Bircher et al., 2013). Nevertheless, changes in the water film thickness due to evaporation has a detectible effect on the amplitude of the signal recorded by the photodetector. Besides changes in light scattering, the transmitted light signal is also affected by interferences between light waves reflected at the surfaces of the thin film (Fig. 2). As water evaporates, the signal increases approximately linearly, until a specific layer thickness is reached where it starts to increase sharply. We attribute this positive peak to constructive interference of the almost perpendicular beam at the layer thickness, $d \simeq \lambda/(2n)$, for wavelength $\lambda = 780$ nm and $n_{780} = 1.329$ (Hale and Querry, 1973). A negative peak directly follows the positive peak as expected from destructive interference. As detailed in Supporting Information S3 section II, a laser diode with an emission peak at around 405 nm instead of at 780 nm was used to prove that the observed signal behavior (Fig. 2) was primarily due to interference effects. Once a specific user-defined threshold of the signal relative to the absolute signal obtained with the dry grid (see Fig. 2 for an explanation) is reached, the pick-and-plunge mechanism is triggered by the monitoring system, whereby the cryo-grid is rapidly vitrified.

Note that the "dry signal" depends on the grid type and mesh size. As the difference is significant, a "blank" measurement always needs to be made before sample deposition (Fig. 2). By contrast, the signal does not depend on the type of sample deposited on a specific grid type/mesh, making it possible to perform screening runs using buffer alone (without sample) to determine the ideal freezing conditions for the experiment.

3.3. Proof of concept cryo-grid preparation from different samples

The examples in this and the following section show that the cryoWriter setup can be used to prepare high-quality cryo-EM grids of different biological samples (e.g., soluble or membrane protein particles, filamentous assemblies, viruses, cell lysate) for various purposes, such as structure determination by single particle analysis (demonstrated below) or helical analysis, and single-cell visual proteomics (Engel, 2010). In practice, the choice of the deposition protocol used for a specific sample depends on its properties and the aim of the experiment. The method is not sensitive to the buffer system employed, as shown in later sections.

The use of the cryoWriter and deposition protocol 1 to spread a 20 nL sample volume on a glow-discharged holey carbon film is demonstrated in Fig. 3. For all preparation steps, the DP-stage temperature was kept 8 °C above the dew point. Subsequently, excess sample was re-aspirated and sample-thinning was performed for 1 s before plunge-freezing. As documented by Fig. 3a, the sample that remained after re-aspiration formed a homogeneous vitreous ice layer covering a part of the cryo-grid; the periphery of the region is visible and indicated by arrows. The homogeneity of the layer is confirmed by Fig. 3b, which shows the holey carbon film at higher magnification to demonstrate that the sample layer spans the holes of the carbon support. Fig. 3c shows the high quality of the apoferritin particles (ring-like appearance) and bacteriophages prepared by this method. The architecture of the bacteriophage tail is revealed (inset). Note the absence of crystalline ice structures, indicating that the sample layer on the grid is indeed vitrified. Further examples are shown in the single particle processing section and in Supporting Information S4.

The use of the cryoWriter and deposition protocol 2 to distribute 3 nL of sample onto a glow-discharged holey carbon film is demonstrated in Fig. 4. Sample thinning was performed by monitored water evaporation as detailed in the dedicated section above. Fig. 4a shows an overview of a typical grid. The area covered by the vitreous sample is generally smaller than the area covered when deposition protocol 1 is used. Furthermore, the thickness of the vitrified sample-layer is not as homogenous (compare Figs. 4 and 3a and b); although the patterned liquid regions deposited by protocol 2 spread out on the hydrophilic grid, a thickness gradient remains due to the surface tension and because water evaporates faster at the periphery of the wet areas. The lower evaporation rate at the center of the sample area is probably a

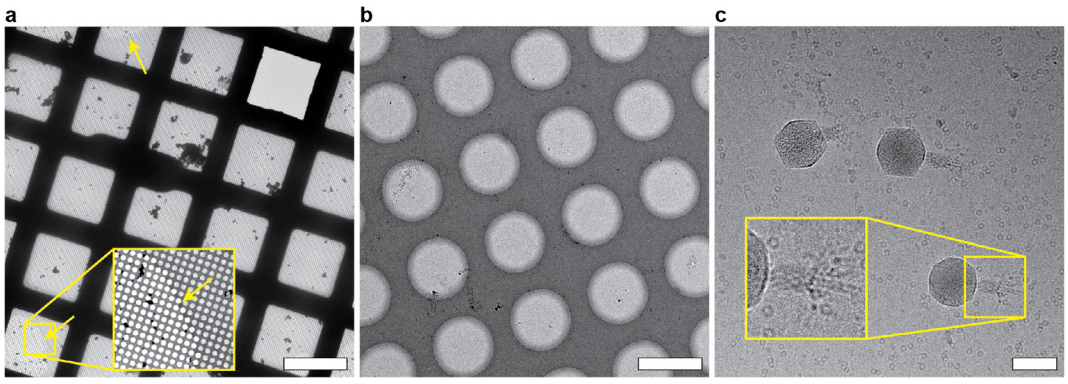

Fig. 3. Proof-of-concept data for cryo-EM grid preparation using the cryoWriter device and deposition protocol 1. A total sample volume of 20 nL was applied to a Quantifoil Cu 200 mesh R2/1 grid; excess liquid was re-aspirated to recover as much sample as possible. The DP-stage temperature was 8 °C above the dew point at all times, which resulted in rapid sample thinning; the grid pick-and-plunge mechanism was automatically triggered immediately after re-aspiration of excess sample. (a) Typical overview of a prepared grid showing a thin film of vitreous ice. Yellow arrows indicate its borders. Inset: fourfold enlargement of a border region after contrast adjustment to improve visibility. Note the continuous and homogenous layer of vitreous sample. Scale bar: 100 μm. (b) Higher magnification overview image demonstrating that the sample layer in the holes is homogeneous. Scale bar: 2 μm. (c) Apoferritin particles and bacteriophages in Tris-HCl buffer prepared by this method and imaged at high magnification and defocus to increase contrast. Inset: twofold enlargement of the indicated region showing a bacteriophage tail and a few ring-shaped apoferritin complexes. Scale bar: 80 nm.

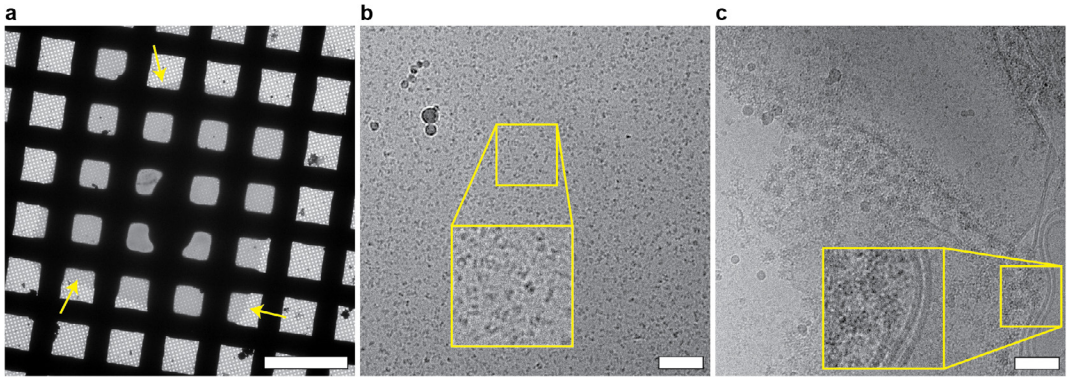

Fig. 4. Proof-of-concept data for cryo-EM grid preparation using the cryoWriter device and deposition protocol 2. In each case, a 3 nL sample volume was directly applied to the grid; no sample was re-aspirated. The grid was vitrified after sample thinning by controlled water evaporation. (a) Overview image of a 3 nL sample volume (urease in PBS buffer) in the middle of a Quantifoil Cu 400 mesh R2/2 grid. Note that the layer thickness has a gradient in some regions. The periphery of the vitreous ice is indicated by yellow arrows. Scale bar: 100 µm. (b) Image of a delicate 200 kDa membrane protein reconstituted in amphipols. Inset: twofold enlargement of the indicated region clearly showing the protein particles. Scale bar: 80 nm. See Supporting Information S5 for a comparison with other sample preparation methods. (c) Example of lossless cryo-grid preparation of the lysate from a single adherent eukaryotic cell. An individual HEK cell growing on a functionalized ITO light microscopy slide was lysed by electroporation and quickly aspirated in a total volume of 3 nL. Subsequently, the lysate was dispensed on the grid using protocol 2 and vitrified. Scale bar: 80 nm.

consequence of the larger surface/volume ratio at the droplet periphery, a transiently higher humidity above the grid due to evaporated water and because the less efficient compensation of the evaporation-induced cooling by heat-flow from the grid to the sample droplet in the center.

The thickness gradients observed when protocol 2 is applied to holey carbon films are a drawback. They could be minimized for some samples by using traces of surfactants, or reduced to a lesser extent for all samples by using EM grids covered with thin continuous carbon films (see Supporting Information S6). However, this is not essential. Cryo-EM can be performed on samples with slightly uneven ice thickness, as demonstrated by Fig. 4b and c. An image of a 200 kDa membrane protein stabilized with amphipols recorded from a holey carbon cryo-grid prepared using the cryoWriter and protocol 2 is shown in Fig. 4b. Images of the same protein prepared on thin carbon film for negative-stain TEM and on

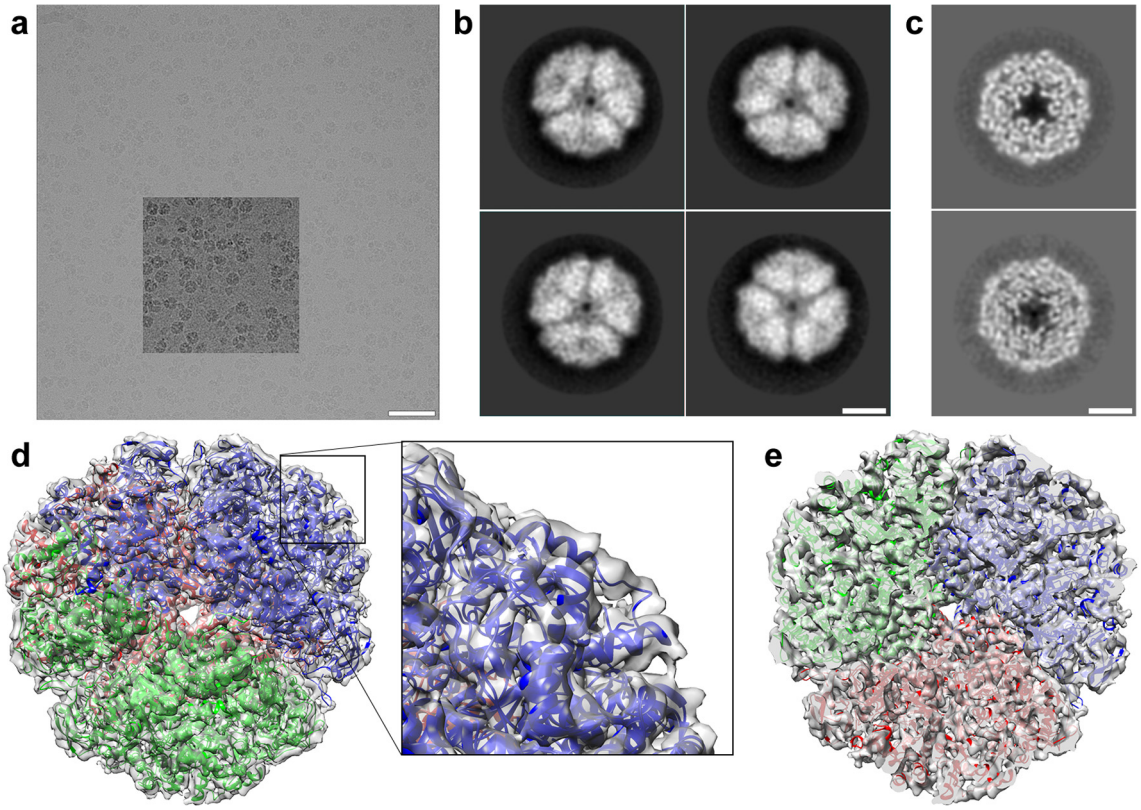

Fig. 5. Use of the cryoWriter to prepare samples for high-resolution structural analysis; proof-of-concept. A 20 nL volume of urease in PBS buffer was deposited on a Quantifoil Cu 200 mesh R1.2/1.3 grid using deposition protocol 1. (a) Drift-corrected cryo-EM image of urease particles embedded in vitreous ice. Inset: the particles with increased contrast. Scale bar, 50 nm. (b) 2D class averages including ~3400 of the 10,000 particles initially selected. Scale bar, 5 nm. (c) 3D class averages including ~5370 of the 8700 particles identified for further processing. Scale bar, 5 nm. (d) Urease density map at 5.03 Å resolution, viewed perpendicular to its threefold axis; the backbone of the fitted X-ray model is shown (DOI: 10.2210/pdb4z42/pdb). (e) A cross-section of the urease density map and the fitted X-ray model perpendicular to the threefold symmetry axis.

lacey and holey carbon for cryo-EM using either a Vitrobot plunge-freezer or the cryoWriter, are shown in Supporting Information S5. Whereas the negative stain image shows intact single particles, degraded particles are found regularly on the grid prepared for cryo-EM by the classic plunge-freezing approach, potentially due to the blotting step. By contrast, the cryo-EM grid prepared with the cryoWriter exhibits a higher protein particle concentration and a higher proportion of homogeneous particles than grids prepared using the classic plunge-freezing approach.

The minute volume consumed when deposition protocol 2 is used, allows cryo-grid preparation from samples that are otherwise inaccessible. For example, the lysate of a single eukaryotic cell can be examined. To demonstrate this, adherent HEK 293 cells were cultured on conducting glass slides and an individual target cell was identified in a light-microscope, electroporated and aspirated using a microcapillary as described previously (Arnold et al., 2016; Kemmerling et al., 2013). The same platinum-coated microcapillary was used for electroporation, cell lysate aspiration and dispensing, thus minimizing the exposure of the tiny amount of biological material to surfaces and the resulting loss of cellular components. Lysate deposition using protocol 2 gave high-quality cryo-grids as shown by Fig. 4c and typical membrane structures with associated proteins are visible. More examples of single cell lysate prepared using sample deposition protocol 2 are shown in Supporting Information S6.

It's difficult to quantify the amount of water that evaporates before plunge-freezing, despite we can monitor the layer thickness. First, the area covered with sample during the deposition process is larger (approx. 0.5 mm^2) than the vitreous ice area observed in the EM, most prominent using deposition protocol 2 (vitreous sample area approx. 0.1 mm^2; Fig. 4a). Second, the dry areas of the grid show traces of sample, indicating that salts and protein also spread to these regions and were not collected and concentrated in the remaining thin vitreous layer on water evaporation. This will always be the case when the substrate is hydrophilic. Note that slight water evaporation from the sample is crucial to obtain thin sample layer suitable for cryo-EM in general (see also the discussion).

3.4. Single particle analysis

In order to demonstrate the usefulness of the cryoWriter method for high-resolution structural analysis, urease from *Yersinia enterocolitica* bacteria was prepared for cryo-EM using deposition protocol 1, and imaged with a Titan Krios microscope equipped with a DED camera (see Section 2). Fig. 5a documents the high quality of the sample grid. Class averages selected from an initial 2D classification are shown in Fig. 5b. Subsets of particles were selected from the classes generated and used in the final processing steps (Fig. 5c). Refinement using two fully independent sub-populations of particles, the so-called "gold-standard" method (Henderson et al., 2012; Scheres and Chen, 2012), yielded a 3D reconstruction of the tetrameric complex at a resolution of 5.03 Å according to the Fourier shell correlation (FSC = 0.143, Supporting Information S7).

4. Discussion

This work was motivated by the need for improved sample-grid preparation methods for cryo-EM and the need to prepare such grids using minimal amounts of sample (nanoliters). The cryo-EM sample deposition and vitrification tool described here only consumes 3–20 nL of sample per grid and can be used together with different types of sample, e.g., single particle preparations of soluble and membrane proteins, viruses and bacteriophages, or whole cell lysate. The setup includes a monitoring system to allow controlled thinning of sample films and the automatic activation of the pick-and-plunge mechanism once a defined threshold is reached. Importantly, freezing conditions and this thickness threshold can be determined using grids prepared with buffer alone instead of the actual sample.

Other important aspects are that the cryoWriter method works with minimal sample loss and does not involve any paper blotting steps. The experience of many laboratories that rely on cryo-grid preparations shows that classic preparation methods can be detrimental to the preservation of delicate protein complexes. This is often attributed to the paper blotting step or to the large surface to volume ratio of the sample film after blotting. The former can rapidly change the buffer characteristics of the sample (salt, pH changes, ions leached from the filter paper) and can also lead to shear forces disturbing long protein assemblies (Lee et al., 2012). The latter exposes more protein to a harsh air-water interface during and after blotting. The sample deposition protocols presented here avoid paper blotting entirely. Deposition protocol 1 also minimizes the time the protein remaining on the grid after sample re-aspiration is exposed to the air-water interface; if the DP-stage offset is +8 °C, samples can be vitrified immediately after deposition. Exposure to the air-water interface is longer when deposition protocol 2 is used; sample deposition, spreading, and thinning can take up to 10 s before the grid enters the cryogen. Both deposition protocols also allow the use of additives, such as traces of detergent, that concentrate at the air-water interface and might protect proteins from surface effects. Sample conditioning by a diffusion driven process (Arnold et al., 2016) can be included in the cryoWriter setup, allowing detergent to be rapidly introduced to small sample volumes (<5 nL) and the preparation of homogeneous grids by protocol 2 (Arnold et al., 2016).

Water evaporation from the sample to obtain thin specimen layers is a critical step during cryo-EM grid preparation. To our experience, water evaporation is also crucial when conventional methods are employed, i.e., in the last stages of paper blotting and in the time interval before plunge-freezing. The question of how much water can be evaporated from a sample without generating harmful conditions for the sample or negatively affecting image quality does not have a general answer. The amount will depend on the protein and the salts present. If the EM images have a grainy background, arising from high salt concentration (see supporting information S4), the cryoWriter protocols can be combined with a conditioning and desalting process described previously (Arnold et al., 2016).

The cryoWriter method promises to significantly shorten the time and effort required to determine suitable freezing conditions. The almost lossless preparation and low sample consumption achieved, will make cryo-EM applicable to the structural analysis of sparsely available proteins/protein complexes and the content of single cells. This is of particular interest because technical advances in cryo-EM now allow resolutions between 3 and 6 Å to be reached by single particle imaging and the analysis of only a few thousand to a few million protein complexes (Liao et al., 2013), making microfluidic sample preparation methods for structural analysis feasible (Giss et al., 2014).

Competing financial interests

The authors declare the following competing financial interest: the cryoWriter concept is part of patent application PCT/EP2015/065398 and EP16194230.

Acknowledgements

We thank the workshop of the Biozentrum of the University Basel for their support, N. Taylor for his help with image processing,

S. Müller for critical discussions and for carefully reading the manuscript, R. Sütterlin for help with cell culturing, A. Fecteau-LeFebvre for technical assistance with EM, J. Senn for assisting with EM data collection, and M. Chami for expert discussions about cryo-EM sample preparation (all from the C-CINA, Biozentrum, University of Basel). We thank A. Engel, emeritus University Basel now University of Delft, Netherlands, for his inspiring conversations. Test samples were kindly provided by P. Ringler, M.-A. Mahi, and T. Schwede (Biozentrum, University of Basel), P. Leiman (Laboratory of Structural Biology and Biophysics, EPFL) and R. Diaz-Avalos (New York Structural Biology Center, USA). The project was supported by the Swiss Nanoscience Institute (SNI, project P1201) and the Swiss National Science Foundation (SNF, project 200021_162521).

Appendix A. Supplementary data

Supplementary data associated with this article can be found, in the online version, at http://dx.doi.org/10.1016/j.jsb.2016.11.002.

References

Arnold, S.A., Albiez, S., Opara, N., Chami, M., Schmidli, C., Bieri, A., Padeste, C., Stahlberg, H., Braun, T., 2016. Total sample conditioning and preparation of nanoliter volumes for electron microscopy. ACS Nano 10, 4981–4988.

Baker, L.A., Rubinstein, J.L., 2010. Radiation damage in electron cryomicroscopy. Methods Enzymol. (chapter fifteen)

Bircher, B.A., Lang, H.-P., Duempelmann, L., Gerber, C., Braun, T., 2013. Photothermal excitation of microcantilevers in liquid: effect of the excitation laser position on temperature and vibrational amplitude. Micro Nano Lett. 8, 770–774.

Callaway, E., 2015. The revolution will not be crystallized: a new method sweeps through structural biology. Nature 525, 172–174.

Dubochet, J., Adrian, M., Chang, J.J., Homo, J.C., Lepault, J., McDowall, A.W., Schultz, P., 1988. Cryo-electron microscopy of vitrified specimens. Q. Rev. Biophys. 21, 129–228.

Elliott, C., Vijayakumar, V., Zink, W., Hansen, R., 2007. National Instruments LabVIEW: a programming environment for laboratory automation and measurement. JALA 12, 17–24.

Engel, A., 2010. Assessing Biological Samples with Scanning Probes. In: Gräslund, A. et al. (Eds.), Single Molecule Spectroscopy in Chemistry, Physics and Biology. Springer Berlin Heidelberg, Berlin, Heidelberg, pp. 417–431.

Giss, D., Kemmerling, S., Dandey, V., Stahlberg, H., Braun, T., 2014. Exploring the interactome: microfluidic isolation of proteins and interacting partners for quantitative analysis by electron microscopy. Anal. Chem. 86, 4680–4687.

Glaeser, R.M., 2016. How good can cryo-EM become? Nat. Methods 13, 28–32.

Grigorieff, N., 2007. FREALIGN: high-resolution refinement of single particle structures. J. Struct. Biol. 157, 117–125.

Hale, G.M., Querry, M.R., 1973. Optical constants of water in the 200-nm to 200-μm wavelength region. Appl. Opt. 12, 555–563.

Henderson, R., Sali, A., Baker, M.L., Carragher, B., Devkota, B., Downing, K.H., Egelman, E.H., Feng, Z., Frank, J., Grigorieff, N., Jiang, W., Ludtke, S.J., Medalia, O., Penczek, P.A., Rosenthal, P.B., Rossmann, M.G., Schmid, M.F., Schröder, G.F., Steven, A.C., Stokes, D.L., Westbrook, J.D., Wriggers, W., Yang, H., Young, J., Berman, H.M., Chiu, W., Kleywegt, G.J., Lawson, C.L. 2012. Outcome of the first electron microscopy validation task force meeting. Structure (London, England: 1993), 20, 205–214.

Jain, T., Sheehan, P., Crum, J., Carragher, B., Potter, C.S., 2012. Spotiton: a prototype for an integrated inkjet dispense and vitrification system for cryo-TEM. J. Struct. Biol. 179, 68–75.

Kemmerling, S., Ziegler, J., Schweighauser, G., Arnold, S.A., Giss, D., Müller, S.A., Ringler, P., Goldie, K.N., Goedecke, N., Hierlemann, A., Stahlberg, H., Engel, A., Braun, T., 2012. Connecting μ-fluidics to electron microscopy. J. Struct. Biol. 177, 128–134.

Kemmerling, S., Arnold, S.A., Bircher, B.A., Sauter, N., Escobedo, C., Dernick, G., Hierlemann, A., Stahlberg, H., Braun, T., 2013. Single-cell lysis for visual analysis by electron microscopy. J. Struct. Biol. 183, 467–473.

Kuhlbrandt, W., 2014. Biochemistry. The resolution revolution. Science 343, 1443–1444.

Lee, J., Saha, A., Pancera, S.M., Kempter, A., Rieger, J., Bose, A., Tripathi, A., 2012. Shear free and blotless cryo-TEM imaging: a new method for probing early evolution of nanostructures. Langmuir 28, 4043–4046.

Lepault, J., Booy, F.P., Dubochet, J., 1983. Electron microscopy of frozen biological suspensions. J. Microsc. 129, 89–102.

Liao, M., Cao, E., Julius, D., Cheng, Y., 2013. Structure of the TRPV1 ion channel determined by electron cryo-microscopy. Nature 504, 107–112.

Lyumkis, D., Brilot, A.F., Theobald, D.L., Grigorieff, N., 2013. Likelihood-based classification of cryo-EM images using FREALIGN. J. Struct. Biol. 183, 377–388.

McLeod, R.A., Kowal, J., Ringler, P., Stahlberg, H., submitted. Robust image alignment for cryogenic transmission electron microscopy.

Milazzo, A.-C., Cheng, A., Moeller, A., Lyumkis, D., Jacovetty, E., Polukas, J., Ellisman, M.H., Xuong, N.-H., Carragher, B., Potter, C.S., 2011. Initial evaluation of a direct detection device detector for single particle cryo-electron microscopy. J. Struct. Biol. 176, 404–408.

Nogales, E., 2015. The development of cryo-EM into a mainstream structural biology technique. Nat. Methods 13, 24–27.

Pettersen, E.F., Goddard, T.D., Huang, C.C., Couch, G.S., Greenblatt, D.M., Meng, E.C., Ferrin, T.E., 2004. UCSF Chimera – a visualization system for exploratory research and analysis. J. Comput. Chem. 25, 1605–1612.

Ramakrishnan, C., Bieri, A., Sauter, N., Roizard, S., Ringler, P., Müller, S.A., Goldie, K. N., Enimanev, K., Stahlberg, H., Rinn, B., Braun, T., 2014. OpenBEB: open biological experiment browser for correlative measurements. BMC Bioinform. 15, 84.

Razinkov, I., Dandey, V.P., Wei, H., Zhang, Z., Melnekoff, D., Rice, W.J., Wigge, C., Potter, C.S., Carragher, B., 2016. A new method for vitrifying samples for cryoEM. J. Struct. Biol. 195, 190–198.

Rohou, A., Grigorieff, N., 2015. CTFFIND4: fast and accurate defocus estimation from electron micrographs. J. Struct. Biol. 192, 216–221.

Ruskin, R.S., Yu, Z., Grigorieff, N., 2013. Quantitative characterization of electron detectors for transmission electron microscopy. J. Struct. Biol. 184, 385–393.

Scheres, S.H., 2012. RELION: implementation of a Bayesian approach to cryo-EM structure determination. J. Struct. Biol. 180, 519–530.

Scheres, S.H.W., Chen, S., 2012. Prevention of overfitting in cryo-EM structure determination. Nat. Methods 9, 853–854.

Tang, G., Peng, L., Baldwin, P.R., Mann, D.S., Jiang, W., Rees, I., Ludtke, S.J., 2007. EMAN2: an extensible image processing suite for electron microscopy. J. Struct. Biol. 157, 38–46.

Tivol, W.F., Briegel, A., Jensen, G.J., 2008. An improved cryogen for plunge freezing. Microsc. Microanal. 14, 375–379.

Veesler, D., Campbell, M.G., Cheng, A., Fu, C.-Y., Murez, Z., Johnson, J.E., Potter, C.S., Carragher, B., 2013. Maximizing the potential of electron cryomicroscopy data collected using direct detectors. J. Struct. Biol. 184, 193–202.